Differential regulation of metzincins in experimental chronic renal allograft rejection: Potential markers and novel therapeutic targets

CC Berthier[1,2,8], N Lods[1,8], SA Joosten[3], C van Kooten[3], D Leppert[4], RLP Lindberg[4], A Kappeler[5], F Raulf[6], EE Sterchi[7], D Lottaz[7] and H-P Marti[1]

[1]Division of Nephrology/Hypertension, Inselspital, University of Bern, Bern, Switzerland; [2]Division of Nephrology, University Hospital of Zürich, Zürich, Switzerland; [3]Department of Nephrology, Leiden University Medical Center, Leiden, The Netherlands; [4]Department of Neurology, University of Basel, Basel, Switzerland; [5]Institute of Pathology, University of Bern, Bern, Switzerland; [6]Department of Transplantation, Novartis Institutes of BioMedical Research, Basel, Switzerland and [7]Institute of Biochemistry and Molecular Biology, University of Bern, Bern, Switzerland

Chronic renal allograft rejection is characterized by alterations in the extracellular matrix compartment and in the proliferation of various cell types. These features are controlled, in part by the metzincin superfamily of metallo-endopeptidases, including matrix metalloproteinases (MMPs), a disintegrin and metalloproteinase (ADAM) and meprin. Therefore, we investigated the regulation of metzincins in the established Fisher to Lewis rat kidney transplant model. Studies were performed using frozen homogenates and paraffin sections of rat kidneys at day 0 (healthy controls) and during periods of chronic rejection at day +60 and day +100 following transplantation. The messenger RNA (mRNA) expression was examined by Affymetrix Rat Expression Array 230A GeneChip and by real-time Taqman polymerase chain reaction analyses. Protein expression was studied by zymography, Western blot analyses, and immunohistology. mRNA levels of MMPs (MMP-2/-11/-12/-14), of their inhibitors (tissue inhibitors of metalloproteinase (TIMP)-1/-2), ADAM-17 and transforming growth factor (TGF)-β1 significantly increased during chronic renal allograft rejection. MMP-2 activity and immunohistological staining were augmented accordingly. The most important mRNA elevation was observed in the case of MMP-12. As expected, Western blot analyses also demonstrated increased production of MMP-12, MMP-14, and TIMP-2 (in the latter two cases as individual proteins and as complexes). In contrast, mRNA levels of MMP-9/-24 and meprin α/β had decreased. Accordingly, MMP-9 protein levels and meprin α/β synthesis and activity were downregulated significantly. Members of metzincin families (MMP, ADAM, and meprin) and of TIMPs are differentially regulated in chronic renal allograft rejection. Thus, an altered pattern of metzincins may represent novel diagnostic markers and possibly may provide novel targets for future therapeutic interventions.

Kidney International (2006) **69,** 358–368. doi:10.1038/sj.ki.5000049

KEYWORDS: chronic rejection; matrix metalloproteinases; meprin; metzincins; renal allograft; tissue inhibitors of metalloproteinases

The two main causes responsible for late renal allograft failure are chronic rejection, a major contributor to chronic allograft nephropathy, and patient death with a functioning transplant.[1] Therapy and precise diagnosis of chronic rejection remain difficult. Therefore, the definition of new diagnostic markers and of novel therapeutic targets continue to be of great clinical relevance.

Alterations in the extracellular matrix (ECM) compartment and in the proliferation rates of various cell types are key features in chronic allograft nephropathy, including chronic rejection processes.[2] The metabolism of ECM proteins in the kidney is influenced substantially by the metzincin superfamily of metalloendopeptidases, notably by matrix metalloproteinases (MMPs)[3,4] and to some extent also by meprin[5–7] and by a disintegrin and metalloproteinases (ADAMs).[8,9]

MMPs are traditionally classified into four categories, namely interstitial collagenases (MMP-1/-8/-13), gelatinases (MMP-2/-9), stromelysins (MMP-3/-7/-10/-11/-12) and membrane-type -MMP (MMP-14/-15/-16/-17).[10,11]

The main function of MMPs is the degradation of ECM proteins and to a lesser extent the regulation of cell proliferation.[4,12–14] Reversible MMP inhibition occurs by their natural inhibitors, tissue inhibitors of metalloproteinases (TIMPs).[15] MMPs represent important mediators in inflammatory diseases and also in tumor invasion, kidney morphogenesis and bone turnover.[3,11,16–20]

MMPs may act as proinflammatory mediators in allograft rejection in several ways: direct tissue injury,[10,11] augmenta-

Correspondence: *H-P Marti, Division of Nephrology/Hypertension, Inselspital Bern, 3010 Bern, Switzerland. E-mail: hpmarti@bluewin.ch*

[8]Both these authors contributed equally to this investigation.

Received 25 May 2004; revised 24 June 2005; accepted 11 August 2005

tion of cell proliferation and/or migration[4,14,21] and facilitation of tissue invasion by extrinsic cells (e.g. leukocytes).[20]

Meprin represents either a cell-surface bound or a secreted zinc endopeptidase of the astacin family of the metzincins.[5–7,22] This protease is composed of α and β subunits of approximately 85–110 kDa, respectively, that form homo- and hetero-oligomeric complexes.[7,23] Rat meprin A exists either as homo-oligomers of α subunits or as heterodimers or tetramers of α and β subunits.[7,23] On the contrary, rat meprin B consists essentially of homo-oligomeric β subunits.[7,23] Only the homo-oligomers of meprin A are secreted proteins.[7] Meprin B and hetero-oligomers of meprin A remain membrane bound.[7]

Meprin is highly regulated and is strongly expressed at the brush border membranes of renal proximal tubular cells and intestinal epithelial cells.[5,24] Meprin cleaves a wide range of peptides and proteins, including collagen type IV, laminin, fibronectin, and nidogen.[22–25]

With respect to the kidney, meprin has been investigated in experimental ischemia and reperfusion injury.[5,26] Mice expressing lower meprin A levels in the kidney showed a decreased degree of renal damage as a result of ischemia and reperfusion.[27] Meprin was found to be cytotoxic to renal tubular epithelial cells and its inhibition by actinonin ameliorated ischemia–reperfusion injury in rats.[5]

The ADAMs represent a family of membrane proteins containing a disintegrin and metalloprotease domain.[8,9] The main substrates of ADAM are integral membrane or ECM proteins. Altered ADAM expression has been found in several disorders including asthma, arthritis, Alzheimer's disease, atherosclerosis, and malignancy.[8,9] We focused on ADAM-17 (tumour necrosis factor-α converting enzyme) due to its prominent role in inflammation.[28]

In our present studies, we analyzed the regulation of a wide spectrum of metzincins in the Fisher (F344) to Lewis (LEW) kidney transplant model.[29,30] Two time points of chronic rejection were chosen, days +60 and +100 after transplantation.[29,30]

RESULTS

F344 to LEW renal transplant model

For our studies, we used the well-established F344 to LEW kidney transplant model. This experimental model has been extensively described in the past.[29,30] Importantly, LEW recipients develop acute rejection at approximately day +25 for several days, followed by chronic rejection beyond day +50 after transplantation. Chronic rejection is characterized by severe histological alterations as well as by increases in microalbuminuria and serum creatinine levels, as shown in Figure 1 and Table 1, and as previously reported.[29,30]

Affymetrix GeneChip analysis

Results of Affymetrix Rat Expression Array 230A GeneChip analysis are summarized in Table 2. Significant upregulation was observed for MMP-11/-12/-14, ADAM-17, TIMP-1/-2 and transforming growth factor (TGF)-β1 during chronic rejection at day +60 and day +100 (with the exception of ADAM-17 and MMP-11). Levels of these two proteases failed to reach statistical significance at a later time point (day +100).

In contrast, MMP-9 and meprin α messenger RNA (mRNA) substantially decreased as a result of the chronic rejection process at both time points and MMP-24 was reduced significantly at day +60.

MMP-2/-3/-7/-8/-10/-16/-23, ADAM-10 and TIMP-3 gene expression remained unchanged during the rejection process.

To complete our studies, we investigated selected metzincin substrates, as shown in Table 2. As expected from the histological alterations commonly seen in chronic allograft rejection and from previous descriptions of our model,[29,30]

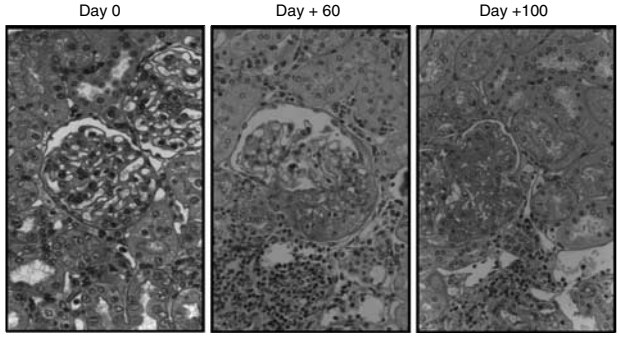

Figure 1 | Renal histology. Left panel: healthy control kidney (day 0). Middle panel: chronic rejection of an F344 renal allograft at day +60 demonstrating glomerular and tubulo-interstitial alterations, as scored in Table 1 (Periodic acid-Schiff staining). Right panel: chronic rejection at day +100 depicting similar histological alterations, as compared to day +60.

Table 1 | Histological and functional characteristics of chronic allograft rejection

	Interstitial infiltrate, tubular atrophy, fibrin in glomeruli, mesangiolysis, glomerulitis	Interstitial fibrosis	Arterial fibrointimal hyperplasia	Microalbuminurea ± s.d. (mg/24 h)	Creatinine (serum) ± s.d. (μmol/l)
Day 0[a]	0[b]	0[b]	0[b]	0.5 ± 0.13	48.67 ± 3.06
Days +60 to +100[c]	2[b]	3[b]	1[b]	10.51 ± 9.74	79.43 ± 10.47

[a] n=8.
[b] Banff classification.[29,31]
[c] n=12 (day +60) and n=6 (day +100).

Table 2 | Affymetrix GeneChip analysis of 25 genes (12 MMP, three TIMP, two ADAM, two meprins, TGF-β1, four collagens, and a proteoglycan core protein) expressed in allografts with chronic rejection (samples at day +60 and day +100) and in healthy kidney controls (samples at day 0)

Gene	RefSeq/GenBank accession no.	Affymetrix probe set	Day 0	Day +60	Day +100
MMP-2	NM_031054	1369825_at	23.8±7.6	18.6±6.3	15.5±4.2
MMP-3	NM_133523	1368657_at	15.7±5.6	18.9±9.6	14.5±7.2
MMP-7 [a]	NM_012864	1368766_at	2.3±1.0[a]	18.5±9.3[a]	8. 7±7. 7[a]
MMP-8	NM_022221	1387735_at	15.6±4. 7	8.2±0.1	7.3±4.6
MMP-9	NM_031055	1398275_at	81.1±29.4	10.5±8.9*	1.3±0.4*[a]
MMP-10[a]	NM_133514	1368713_at	1.2±0.5[a]	1.6±0.1[a]	3.5±4.2[a]
MMP-11	NM_012980	1367858_at	34.7±7.3	76.5±16.7*	41.6±17.8
MMP-12	NM_053963	1368530_at	5.7±4.0[a]	259.6±146.7*	134.7±38.5*
MMP-14	RNMTMMP	1367860_at	77.5±13.4	257.5±82.4*	203.7±55.2*
MMP-16	NM_080776	1368590_at	9.7±11.5	17.3±2.6	5.2±4.4
MMP-23	NM_053606	1368961_at	46.6±4.3	45.4±34.0	38.0±9.0
MMP-24	BF285924	1389833_at	355.0±40.5	190.1±23.3*	256.7±53.4
TIMP-1	NM_053819	1367712_at	54.7±12.1	451.3±163.7*	255.1±156.3*
TIMP-2	NM_021989	1386940_at	181.5±30.9	485.0±77.7*	287.3±99.2*
TIMP-3	NM_012886	1368989_at	77.9±4.7	54.0±6.6	110.4±109.4
ADAM-10	BI300565	1370955_at	18.4±5.0	22.0±1.9	21.0±8.8
ADAM-17	NM_020306	1367922_at	161.5±10.6	273.2±42.8*	183.2±24.2
Mep1α	NM_013143	1368236_at	2124.4±106.8	473.4±515.6*	1074.3±575.0*
Mep1β	NM_013183	1387158_at	1179.9±121.7	343.3±429.2	831.4±478.4
TGF-β1	NM_021578	1370082_at	23.8±3.2	175.6±33.2*	96.0±17.2*
Collagen I α1	BI285575	1388116_at	45.3±6.4	337.1±133.6*	159.2±24.1
Collagen I α2	BI282748	1387854_at	49.4±7.5	208.2±62.1*	137.7±10.2
Collagen III α1	BI275716	1370959_at	95.0±27.4	599.8±254.1*	346.5±42.5
Collagen IV α1	BE111752	1373245_at	357.6±23.5	1145.7±210.2*	658.1±205.9
Proteoglycan core protein	NM_020074	1368655_at	90.1±1.7	278.1±113.7	172.0±28.9

Affymetrix Rat Expression Array 230A GeneChip data, MAS5 normalized expression values (mean±s.d.; n=3 for each group: day 0, day +60 and day +100 after transplantation).
*Significant difference (up or down) compared to day 0 (P-values < 0.05 by multiple group ANOVA analysis).
[a]All absent calls (no expression).

there was a significant upregulation of mRNA collagens I α1, I α2, III α1and IV α1 at day +60.

Subsequently, significant results regarding metzincins were further investigated and confirmed by real-time polymerase chain reaction (PCR) analysis. Despite the negative GeneChip results, we further analyzed MMP-2/-7/-8, TIMP-3 and meprin. MMP-2 is particularly relevant, as it represents one of the most extensively investigated MMP in inflammatory disorders. Owing to the clear trend towards a decrease, meprin β also warranted additional investigations. Because of their biological relevance in inflammation, MMP-7/-8 and TIMP-3 were also included in the real-time PCR analyses.[32]

Because glyceraldehyde-3-phosphate dehydrogenase (GAPDH), represented by three different probe sets on the microarray, was not regulated and remained constant between the three different groups (data not shown), we were able to use it as a housekeeping gene for normalizing data in the subsequent real-time PCR analyses.

Real-time reverse transcriptase-polymerase chain reaction analyses of MMP, TIMP, ADAM-17, and TGF-β1

Affymetrix GeneChip results were validated by real-time quantitative reverse transcriptase-polymerase chain reaction at days 0 ($n=8$), +60 ($n=12$) and +100 ($n=6$). These results are summarized in Figure 2a. The respective native contralateral kidneys from day 0 served as healthy controls and their values are depicted as 1.

During the rejection process, mRNA levels of MMP-2/-11/-14 and particularly MMP-12 increased (approx. 5.2/2.6/2.4/67.7-fold, respectively), as well as TIMP-1/-2 (approx. 10.5/2.5-fold) and ADAM-17 (1.7-fold at day +60). However, MMP-9 decreased (approx. 7.5-fold) and TIMP-3 remained unchanged. As expected, TGF-β1 (positive control) was also augmented (6.8-fold and 4.3-fold at days +60 and +100, respectively). For all these comparisons between day 0 and days +60 or +100, $P<0.05$.

As depicted in Figure 2b, MMP-7 remained below the detection limit in all control samples of day 0 ($n=8$; C_T values $\geqslant 40$). During chronic rejection, MMP-7 was detectable in 10/12 samples at day +60 and in all samples at day +100 ($n=6$). Therefore, MMP-7 was significantly upregulated in chronic allograft rejection at both time points ($P<0.05$).

With regard to MMP-8, half of the control samples from day 0 were below the detection limit ($n=8$; C_T values $\geqslant 40$). At day +60, the results for 10/12 samples were heterogeneous and two samples were below the detection limit. All

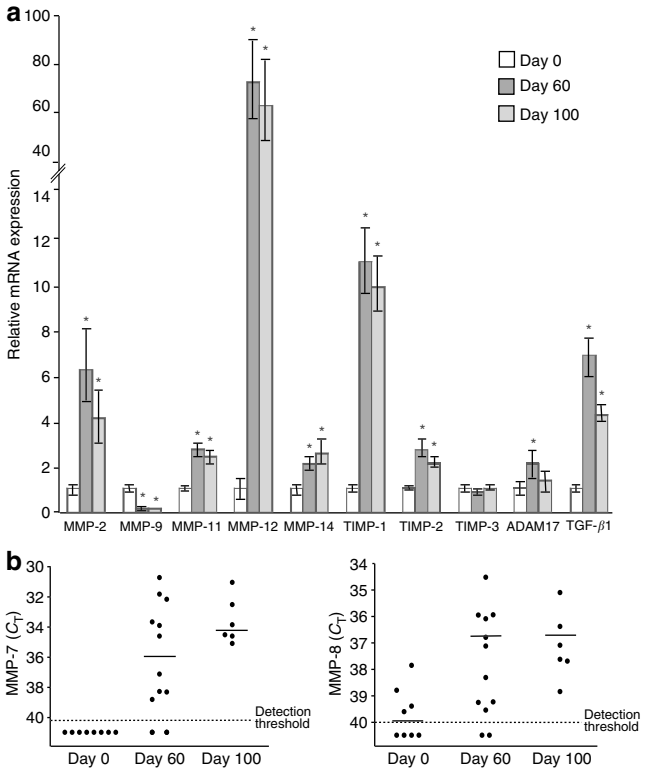

Figure 2 | Relative mRNA levels of MMP, TIMP, ADAM-17, and TGF-β1 by real-time quantitative PCR. (**a**) Overexpression of MMP-2/-11/-12/-14, TIMP-1/-2 and TGF-β1 occurred during chronic rejection at days $+60$ ($n=12$) and $+100$ ($n=6$), compared with the control, at day 0 ($n=8$). Furthermore, an upregulation of ADAM-17 was significant at day $+60$. Although MMP-9 decreased during chronic rejection, TIMP-3 remained unchanged. The mRNA levels were normalized to GAPDH, calibrated to day 0 values (*x*-fold) (control = 1). *$P<0.05$ compared with the control group. (**b**) All MMP-7 and half of the MMP-8 values in control samples were below the detection limit with C_T values $\geqslant 40$. Nevertheless, MMP-7 and MMP-8 were clearly detectable in most cases of chronic rejection. Horizontal bars indicate medians of all samples per group. $P<0.05$ compared with the control group.

samples expressed MMP-8 at day $+100$ ($n=6$). Also, MMP-8 was significantly increased at both time points of chronic allograft rejection ($P<0.05$).

In general, the quantitative real-time PCR data reflect the results obtained by the less quantitative GeneChip analysis with the exception of two out of 12 genes, MMP-2 and MMP-8. While MMP-8 is a low expressed gene with some variability, as shown in Figure 2b, the discrepancy with MMP-2 was further investigated.

Using a second primer/probe set taken from a different gene location, we confirmed the increase in MMP-2 mRNA level obtained by real-time PCR (Figure 2a),[33] as described in the Materials and Methods section. We obtained identical results as compared to the first primer/probe set (data not shown).

Thus, we explained the discrepancies in the results for rat MMP-2 expression observed by TaqMan reverse transcriptase-polymerase chain reaction and Affymetrix genechips. Affymetrix probeset 1369825_at is based on 3′ UTR sequence of GenBank entry X71466. Owing to alternative splicing or different processing, this untranslated region of rat MMP-2 is not found in GenBank entry U65656. Therefore, most likely our two TaqMan probes detected all splice variants of rat MMP-2 and the Affymetrix probeset did not recognize the U65656 variant of MMP-2 overexpressed in our rat model of chronic rejection.

Subsequently, we excluded an effect of age on metzincin expression. As we observed the most striking results at day $+60$, we focused on this time point. Real-time PCR analyses showed constant mRNA levels for MMP-2/-9/-12/-14, TIMP-2 and TGF-β1, in healthy F344 rats aged 10 weeks old (corresponding to day 0 of our transplantation model; $n=4$) compared to healthy F344 rats that were 10 weeks and 60 days old ($n=4$); data not shown. In addition, there was also no difference in MMP-2 activity between both groups as determined by zymography (data not shown).

Limited metzincin analyses have also been performed on day $+30$ during the period of acute renal allograft rejection, exactly between day 0 and day $+60$. The aim of these studies was to investigate whether the pattern of metzincin expression differentiates between acute and chronic rejection. Significant upregulation of the following genes was observed in acute graft rejection, as compared to healthy control kidneys from day 0 ($P<0.05$): MMP-2 ($7\times$), MMP-12 ($74\times$), MMP-14 ($7\times$) and TIMP-2 ($14\times$). Again, MMP-9 displayed a marked downregulation ($5\times$; $P<0.05$). These increases or decreases in gene regulation were also observed in chronic rejection, as described. However, the degrees of up- or downregulation of these MMP/TIMP occurred at a significantly higher degree in acute rejection than in chronic rejection at both time points ($P<0.05$ for all comparisons).

Investigation of MMP-2

Results of MMP-2 zymography are depicted in Figure 3a. The upper panel shows a representative zymogram of two samples per investigated group. The higher band at 72 kDa represents pro-MMP-2 and the lower band at 62 kDa depicts the active form of MMP-2.[34] There is clearly a visible increase of MMP-2 activity, especially the pro-form, which can be seen at day $+60$ during the chronic rejection process (lanes 3–4), as compared to controls (lanes 1–2). The high activity levels continued until day $+100$ (lanes 5–6).

The lower panel shows densitometric analysis of all samples (mean $\pm$ s.e.m.), obtained at day 0 ($n=8$), day $+60$ ($n=12$), and day $+100$ ($n=6$), respectively. Each result is expressed as a percentage of the control at day 0 (100%). Pro-MMP-2 activity increased 3.4-fold during rejection at day $+60$ ($P<0.01$) and 2.6-fold at day $+100$ ($P<0.01$), as compared with the control level at day 0. Activity of the MMP-2 fragment had increased almost 1.5-fold at both time points ($P<0.05$).

Endogenous MMP-2 activity was also measured by fluorometric analysis.[35] The respective results (mean $\pm$ s.e.m.) are depicted in Figure 3b. MMP-2 activity at day $+60$ ($n=12$) and day $+100$ ($n=6$) was increased by 47 and 51%, respectively, as compared to the control levels at day 0 ($n=8$)

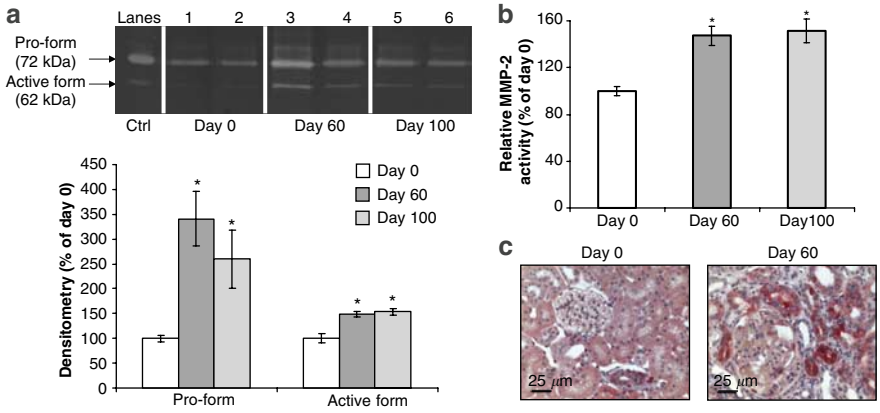

Figure 3 | MMP-2 activity and expression. (**a**) Zymography (upper panel), including densitometry (lower panel), showed increased activities of pro-MMP-2 (72 kDa) and of active MMP-2 (62 kDa) at day +60 (lanes 3–4) and day +100 (lanes 5–6), as compared to the controls of day 0 in lanes 1–2. Ctrl = purified MMP-2 antigen (Calbiochem, Switzerland) as a reference for MMP-2 identification. *$P<0.05$ compared with the control group. (**b**) Fluorometry confirmed increased MMP-2 activity ($n=6$ per group). Each result is expressed as a percentage of the control value at day 0 set at 100%. *$P<0.05$ compared with the control group. (**c**) MMP-2 immunohistology of the kidney sections. The presence of MMP-2 was observed especially in the tubuli, but also to some extent in the glomeruli in case of chronic rejection at day +60 (right), compared to the healthy control demonstrating only a positive staining in an arteriolar blood vessel (day 0, left).

($P<0.05$). Experiments were also performed in the presence of phenylmethyl-sulfonylfluoride and phenantroline to investigate the specificity of our assay (data not shown). As expected, the addition of phenylmethyl-sulfonylfluoride, a serine protease inhibitor, did not influence MMP activity. On the contrary, phenantroline – a zinc-chelator and MMP inhibitor – reduced the activity in all samples to almost zero.

Immunohistological staining of MMP-2 is depicted in Figure 3c. During chronic rejection at day +60, MMP-2 expression is increased, as represented by a stronger staining of the tubuli and to some extent in the glomerulus.

Investigation of MMP-9

MMP-9 protein level was further examined by Western blot, zymography, and histological staining of allograft sections.

Western blot analysis of MMP-9 protein expression is depicted in Figure 4a. We detected two bands (upper panel), one at 130 kDa representing most likely the heterodimer of MMP-9 and its major inhibitor TIMP-1, and another band at 92 kDa corresponding to the pro-form of MMP-9.[36] However, at this stage it cannot be fully excluded that the band observed at 130 kDa may also, in part, represent MMP-9 complexed with N-Gal.[37]

According to densitometric analysis ($n=6$ per group), the heterodimeric complex decreased by approximately 45 and 55% at days +60 and +100, respectively, as compared to day 0 ($P<0.05$). The pro-form of MMP-9 decreased by approximately 35 and 70% at days +60 and +100, respectively, in comparison to day 0 ($P<0.05$). These results are shown in Figure 4a (lower panel).

Immunohistological staining of MMP-9 is depicted in Figure 4b. At day +60, MMP-9 expression is barely detectable during chronic rejection. Strong staining of MMP-9 was detected in the glomeruli of healthy kidney from day 0 (as also shown by others).[38]

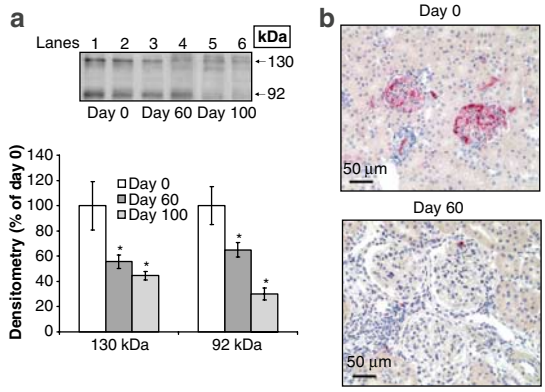

Figure 4 | MMP-9 protein expression. (**a**) Western blot analyses (upper panel), including densitometry (lower panel), showed a decreased presence of MMP-9/TIMP-1 (130 kDa) and of pro-MMP-9 (92 kDa) at days +60 (lanes 3–4) and +100 (lanes 5–6) compared to day 0 (lanes 1–2). *$P<0.05$ compared with the control group. (**b**) Immunohistology in the kidney sections. Negative or minimal staining of MMP-9 in the glomeruli was observed in chronic rejection (day +60, lower), compared to the positive control (day 0, upper). Furthermore, there appears to be some peritubular MMP-9 staining in control tissue.

MMP-9 activity in zymograms of all samples was just at the detection limit and therefore not usable for (semi-) quantitative analysis (data not shown).

MMP-14 and TIMP-2 expression

A decisive role of MMP-14 and TIMP-2 in pro-MMP-2 activation is already well known.[12,34,39,40] Thus, it was of great interest to study MMP-14 and TIMP-2 genes, also at the protein level. The synthesis of MMP-14 was investigated by Western blot analysis, as depicted in Figure 5a, upper panel. MMP-14 was recovered in two different forms, as reflected by the bands at 58 kDa corresponding to the active form of MMP-14 and at 70 kDa reflecting a dimer of MMP-14 and TIMP-2.[12,34,39,40]

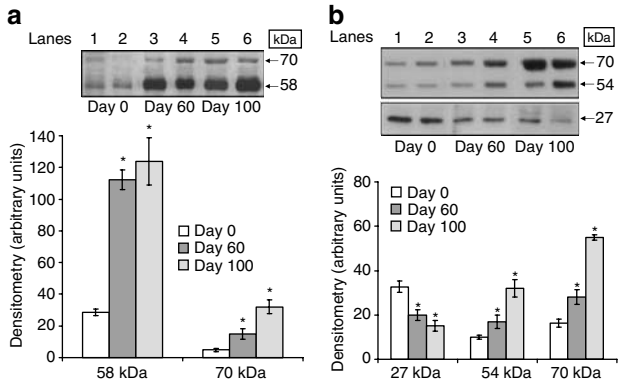

Figure 5 | MMP-14 and TIMP-2 protein expression. (**a**) Upper panel: Western blot analyses of MMP-14 from renal tissues at day 0 (lanes 1–2), day +60 (lanes 3–4), and day +100 (lanes 5–6) after transplantation. Two representative samples for each group are depicted. Lower panel: densitometry of the two bands representing MMP-14 alone or in complex with TIMP-2 in control kidneys ($n=6$) vs kidneys collected at day +60 ($n=6$) and day +100 ($n=6$). The molecular weight of each band of interest is approximately 58 kDa (MMP-14) and 70 kDa (complex of MMP-14/TIMP-2). *$P<0.05$ compared with the control group. (**b**) Upper panel: Western blot analyses of TIMP-2 from renal tissue at day 0 (lanes 1–2), day +60 (lanes 3–4), and day +100 (lanes 5–6) revealed three bands representing TIMP-2, such as 27 kDa (free TIMP-2), 54 kDa (TIMP-2 dimer) and 70 kDa (bimolecular complex of TIMP-2/MMP-14). Two representative samples for each group are depicted. Lower panel: densitometry of these three bands was performed in control kidneys ($n=6$) vs kidneys collected at day +60 ($n=6$) and day +100 ($n=6$). *$P<0.05$ compared with the control group.

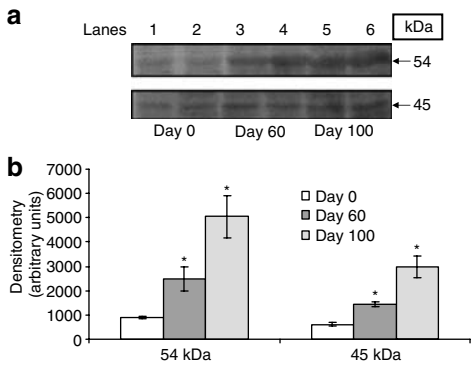

Figure 6 | MMP-12 protein expression. (**a**) Western blot analyses of pro-MMP-12 (54 kDa) and of the intermediate form of MMP-12 (45 kDa) in renal protein extracts from rats at day 0 (lanes 1–2), day +60 (lanes 3–4), and day +100 (lanes 5–6). Representative results of two animals per group are shown. (**b**) The densitometric analyses were performed on three samples for each group. *$P<0.05$ compared with the control group.

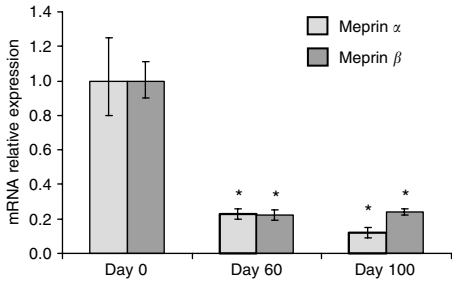

Figure 7 | Meprin α and β mRNA levels during chronic renal allograft rejection. mRNA levels were measured using real-time quantitative PCR in three groups of rats: at day 0 ($n=8$) and during chronic rejection at day +60 ($n=12$) and at day +100 ($n=6$). Meprin mRNA levels decreased during chronic rejection at both time points. Values at day 0 were set to 1. *$P<0.05$ compared with the control group.

In this respect, densitometry revealed that active MMP-14 increased approximately fourfold at day +60 and day +100, as compared to day 0 ($P<0.01$), as depicted in Figure 5a, lower panel. MMP-14 complexed with TIMP-2 showed threefold and sixfold increases at day +60 and day +100, respectively ($P<0.01$).

The presence of TIMP-2 was demonstrated in three different identifiable forms, as shown by Western blot analysis depicted in Figure 5b, upper panel. The free form of TIMP-2 at 27 kDa[40] decreased by 39% (day +60) and 54% (day +100) during chronic rejection ($P<0.05$), as represented by the respective densitometry (Figure 5b, lower panel). The dimeric complex of TIMP-2 at 54 kDa increased approximately 1.7-fold and 3.2-fold during the course of chronic rejection ($P<0.01$). Finally, the bimolecular complex of TIMP-2 and MMP-14 at 70 kDa[40] increased 1.7-fold and 3.4-fold at days +60 and +100, respectively ($P<0.01$). The decrease of free TIMP-2 during chronic rejection was probably due to its extensive recruitment to form complexes.[41]

MMP-12 expression

The upregulation of MMP-12 observed at the mRNA level was further investigated. The protein expression was analyzed by Western blot, as depicted in Figure 6a. Two representative samples of each category (day 0, day +60, day +100) are shown. Pro-MMP-12 of 54 kDa and the intermediate form of MMP-12 of 45 kDa (data sheet, Oncogene, 45) increased by approximately 2.8-fold and 2.4-fold at day +60 and by 5.6-fold and 4.9-fold at day +100 ($P<0.05$), respectively, as depicted in Figure 6b.

Investigation of meprin

To substantiate the GeneChip results for meprin, real-time reverse transcriptase-polymerase chain reaction was performed to analyze meprin α and meprin β mRNA levels during chronic rejection (Figure 7). For comparative analysis, mRNA from non-transplanted kidneys at day 0 served as healthy controls (set to 1.0).

Meprin α mRNA levels decreased to approximately 25 and 10% of controls at day +60 and day +100, respectively ($P<0.05$). Meprin β mRNA decreased to about 25% of controls at both time points ($P<0.05$).

The expression of meprin protein was assessed by Western blot analysis. Two representative samples of each category (day 0, day +60, day +100) are shown for meprin α and for meprin β (Figure 8a, upper panel).

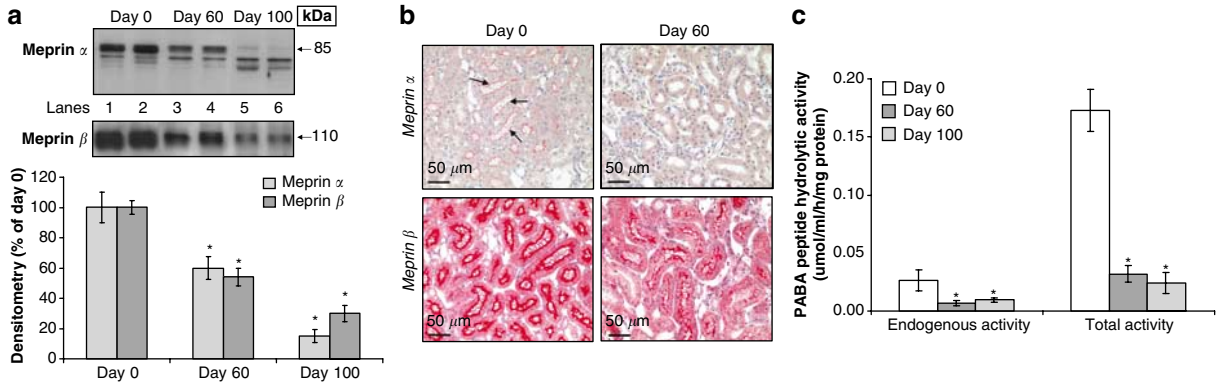

Figure 8 | Meprin protein synthesis. (**a**) Upper panel: Western blot analyses of meprin α (85 kDa) and meprin β (110 kDa) (upper panel) in renal protein extracts from rats at day 0 (lanes 1–2), day +60 (lanes 3–4) and day +100 (lanes 5–6) after transplantation. Representative blots of two animals are shown. Lower panel: the densitometric analyses of the respective blots were performed on six samples per group (day 0, day +60 and day +100). *$P<0.05$ compared with the control group. (**b**) Immunohistology of meprin in renal tissue sections. Stainings for meprin α (upper pictures) and meprin β (lower pictures) in renal tissue sections at day 0 (left pictures) and day +60 after transplantation (right pictures) are represented. Meprin α was present at the brush border membrane of proximal tubular cells of control kidneys (black arrows), but not visible in chronic rejection. Meprin β was detectable in both states, but clearly reduced in chronic rejection. (**c**) Meprin activity. Endogenous activity and total activity (after exogenous activation using trypsin) were assessed with *N*-benzoyl-L-tyrosyl-*p*-aminobenzoic acid as substrate ($n=6$ per group). Meprin activity clearly decreased during phases of chronic allograft rejection at days +60 and +100 after transplantation. *$P<0.05$ compared with the control group.

In kidney tissue, the mature extracellular form of meprin α has been shown to correspond to a molecular mass of 85 kDa.[42,43] In accordance with real-time PCR results, this form of meprin α was reduced during chronic rejection at day +60 (Figure 8a, upper panel, lanes 3–4) and especially at day +100 (lanes 5–6) after transplantation, as compared to controls (day 0, lanes 1–2). Densitometric analysis of six samples in each group is represented below (Figure 8a, lower panel). It shows a reduction of the 85 kDa band by approximately 40 and 85% at day +60 and day +100, respectively ($P<0.01$). Additional bands appeared along the process of chronic rejection at a lower molecular weight, in the order of 75 kDa. The identity of this form of meprin α was not investigated further, but it cannot be excluded that they represent degraded forms of meprin.

The major form of renal meprin β has a molecular mass of 110 kDa. Meprin β expression decreased at day +60 (Figure 8a, upper panel, lanes 3–4) and at day +100 (lanes 5–6) as compared to controls (day 0, lanes 1–2). The densitometric analysis of six samples in each group demonstrated a reduction of meprin β protein levels during chronic rejection by 46% at day +60 and by 70% at day +100 after transplantation ($P<0.01$), as depicted in Figure 8a (lower panel).

As expected, immunohistological staining for meprin α and β in tissue sections of control kidneys at day 0 revealed strong localization of both subunits at the brush border membrane of proximal tubular cells (Figure 8b, left panel). During chronic rejection at day +60, meprin α was not detectable (Figure 8b, upper right picture) and staining for meprin β was significantly weaker (Figure 8b, lower right picture) than in the respective control tissues.

Thus, the downregulation of meprin α and β at the brush border membrane of proximal tubular cells is compatible with the results of mRNA and protein expression described above.

Combined meprin α and β activity was determined using *N*-benzoyl-L-tyrosyl-*p*-aminobenzoic acid as substrate (Figure 8c). The endogenous activity of meprin decreased by approximately 70% at days +60 and +100 after transplantation compared to day 0 (0.008 vs 0.026 μmol/ml/h/mg protein) ($P<0.05$). Meprin is synthesized as a zymogen, which may be activated by trypsin. Therefore, we pretreated protein extracts with trypsin *in vitro* to measure total meprin activity. Total activity was 6.5-fold higher than endogenous activity at day 0 (0.173 vs 0.026 μmol/ml/h/mg protein; $P<0.05$), indicating that only a minor portion of meprin is endogenously active in the kidney *in vivo*. However, during chronic rejection at days +60 and +100, a similar decrease by approximately 80% was observed in the case of total meprin activity (0.03 μmol/ml/h/mg protein; $P<0.05$).

DISCUSSION

The present investigation analyzes the expression and activity of metzincins in chronic renal allograft rejection. These proteases were investigated as they represent a growing superfamily of key regulators of ECM metabolism and of cell proliferation.

We studied three members of the metzincin superfamily: MMP (including TIMP), meprin α/β and ADAM-17. Our findings indicate that MMP/TIMP (with the exception of MMP-9) are upregulated and meprin α/β are downregulated in chronic renal allograft rejection.

In humans, increased circulating levels of MMP-1 were found in subjects with acute kidney allograft rejection, whereas concentrations of MMP-2 and MMP-3 were increased in patients with chronic transplant nephropathy.[44,45]

MMP and TIMP have been investigated in a rat model of acute kidney transplant rejection using a Buffalo donor to a Wistar-Furth recipient.[12] Increased graft levels of pro-MMP-2/

-9/-14 and active MMP-14 but decreased concentrations of activated MMP-2/-9, TIMP-2 and of inactive fragments of MMP-14 were reported.[12] In a previous study, we have investigated the role of MMP in the Dark Agouti to Lewis model of severe acute renal allograft rejection.[46] However, the synthetic MMP inhibitor BB-94 did not show a clear benefit on renal histology and on proteinuria.[46]

Taken together, in severe acute rejection, metzincins may be somewhat redundant due to the magnitude of other activated inflammatory mediators. The role of MMP in chronic renal allograft rejection may be more important, as quantitative and qualitative alterations in the ECM compartment represent the most characteristic findings in this rejection process.

In the present study, we utilized the F344 to LEW rat model of chronic renal allograft rejection.[29,30] LEW recipients of F344 allografts develop acute rejection at around day +25 lasting for several days and leading to graft loss in the order of 50%. The surviving rats demonstrate histological and functional characteristics of chronic rejection from day 50 onwards, without concomitant immunosuppressive treatment.

Chronic renal allograft rejection led to increased mRNA levels of key MMP, such as MMP-2/-11/-12/-14, and their inhibitors, TIMP-1 and TIMP-2. In parallel, we demonstrated increased MMP-2 activity and synthesis. Accordingly, augmented levels of MMP-2 mRNA have been reported by others during chronic allograft nephropathy in humans.[47]

TIMP-2 represents the main inhibitor of MMP-2, but it also forms complexes with MMP-14 to activate MMP-2.[12,34,39,40] Therefore, we investigated TIMP-2 and MMP-14 in more detail. In fact, an increased production of TIMP-2 and MMP-14 alone and in complexes was demonstrated at the protein level.

MMP-12 (metalloelastase) showed the strongest increase of any type of metzincin with an approximately 70-fold augmented mRNA level during chronic allograft rejection. Although the role of MMP-12 in rejection processes remains to be defined, MMP-12 was previously shown to play a role in inflammation. MMP-12 appeared to support leukocyte influx and to be necessary for the development of acute alveolitis in a mice model of lung injury.[48]

Surprisingly, MMP-24, and especially MMP-9, decreased substantially during allograft rejection. To our knowledge, this is a novel finding without any precedence, which warrants further investigation. Nevertheless, due to a relatively low overall expression, MMP-9 appears to represent a marker of rejection processes rather than a pathophysiologic relevant factor. This has been demonstrated in a group of patients with chronic glomerulonephritis, where MMP-2 was found to be increased and MMP-9 to be downregulated.[35]

Among the ADAM family of proteases, we investigated ADAM-17 (tumor necrosis factor-α (TNF-α) converting enzyme). ADAM-17 processes TNF-α and represents a validated therapeutic target for anti-inflammatory interventions.[28,49] In our studies, ADAM-17 clearly increased during chronic renal allograft rejection at day +60. Thus, the inhibition of ADAM-17 offers a new perspective for the treatment or prevention of chronic allograft nephropathy.

In our model, meprin was significantly downregulated as a result of the chronic rejection process. Interestingly, according to the microarray data, meprin was by far the strongest metzincin expressed in healthy control kidneys.

The decrease of meprin was demonstrated at the mRNA level, visualized by microarrays and real-time quantitative PCR, and at the protein level, determined by Western blot, immunohistology and activity tests. The presence of smaller molecular forms of meprin α suggests that this subunit may be partially degraded during rejection. Accordingly, renal meprin activity had decreased substantially. Because meprin is mainly expressed in the brush border of renal tubular cells, the decrease of meprin may be the consequence of tubular alterations or even destructions in chronic renal allograft rejection. However, the increase of TGF-β in chronic rejection may also be in part responsible for the decrease in meprin activity by its inhibitory effect on plasmin activity and stimulatory action on PAI-1 synthesis.[50,51]

The pattern of differentially regulated metzincins may lead to novel diagnostic markers of renal allograft rejection. As an example, this may be relevant for MMP-12 particularly using microarrays, as our Affymetrix GeneChip failed to detect this protease in healthy control kidneys, but showed a very strong signal in chronic rejection. Furthermore, upregulated MMP may also represent individual targets for therapeutic interventions.

According to our limited results, the altered pattern of metzincin expression does not distinguish between acute and chronic renal allograft rejection, although further investigation is warranted to definitely resolve this issue.

As we did not perform an interventional investigation, we cannot determine whether the alterations in metzincin expression are beneficial or detrimental. For future interventions, MMP activity can be inhibited by synthetic MMP inhibitors. We have previously shown that hydroxamate-based MMP inhibitors inhibit cell proliferation and matrix accumulation in analyses of cultured mesangial cells and of anti-Thy1.1 nephritis.[52–54]

Angiotensin-converting enzyme inhibitors also inhibit MMP activity[35] and the angiotensin-converting enzyme inhibitors enalapril ameliorated chronic renal allograft rejection in the F344 to LEW rat strain combination.[55] Thus, a part of the therapeutic benefit of angiotensin-converting enzyme inhibitors may be the consequence of concomitant MMP inhibition.

In conclusion, metzincins, such as MMP, ADAM-17, meprin, and TIMP, are dysregulated in chronic renal allograft rejection. Therefore, metzincins may represent novel diagnostic markers for chronic renal allograft rejection. Furthermore, upregulated MMP, TIMP, and ADAM-17 may provide novel therapeutic targets for the prevention and treatment of chronic rejection processes.

MATERIALS AND METHODS

Animals

Male inbred F344, RT1^{lv1}, and LEW, RT1l rats (250 g body weight) were obtained from Harlan, Horst, The Netherlands.[29,30]

Kidney transplantation

Kidney transplantation was performed by SA Joosten and C van Kooten, as described previously.[29,30] Briefly, the left kidney of the LEW recipient was removed and orthotopically replaced by the F344 donor kidney. The contralateral F344 kidneys of the donor were used as healthy controls of day 0. A patch of the donor aorta and the inferior vena cava was anastomized to the corresponding recipient's blood vessels. Anastomosis of the donor urethra was performed end-to-end. Nephrectomy of the remaining native kidney occurred at day +7 after transplantation. For our analyses, recipients were killed at day 0, day +30, day +60, and day +100 postoperatively.

To exclude an effect of age on metzincin expression, we included an additional control group of healthy F344 rats that were 10 weeks and 60 days old at the time of analysis.

Analysis of renal histology by periodic acid-Schiff staining and of microalbuminuria was performed as described.[29,30] Serum creatinine levels were determined by routine methodology.

RNA isolation

Total RNA was isolated from frozen tissues according to the manufacturer's instructions (RNeasy; Qiagen, Zurich, Switzerland) and stored at −70°C. RNA of high quality was obtained, as assessed by Bioanalyzer 2100 electropherograms (Agilent).

GeneChip expression profiling

DNA microarray analysis was performed using GeneChip hybridization according to the manufacturer's instructions (Affymetrix). Affymetrix Rat Expression Array 230A GeneChips comprise 15 924 probe sets (25mer oligonucleotide probes; 11 probe pairs/set). Briefly, 5 μg total RNA was reversed transcribed into double-strand cDNA in the presence of a $(dT)_{24}$/T7 primer. Labeled cRNA was synthesized by T7 RNA polymerase in the presence of biotinylated ribonucleotides and hybridized overnight to the GeneChips followed by a 2-h washing and staining using streptavidin-coupled phycoerythrin. Finally, each GeneChip was scanned by a laser scanner. The images were processed using the Microarray Analysis Suite (Affymetrix) version 5 (MAS5). All expression experiments were scaled to the same target intensity (150).

Reverse transcription

Total RNA (0.5–1 μg/μl final concentration) was first treated with DNase I (Sigma). One microgram of DNase-treated total RNA was reverse transcribed at 60°C for 1 h in a reaction mixture containing a final concentration of 1 mM of deoxynucleotide triphosphates (Promega), 2.5 μM random hexamer primers, 1× PCR buffer II, 5 mM $MgCl_2$, 1 U/μl RNase inhibitor, and 2.5 U/μl of Murine Leukemia Virus Reverse Transcriptase (Applied Biosystems). Complementary DNA was stored at −20°C until real-time quantitative PCR (TaqMan PCR).

Real-time TaqMan PCR analysis

The PCR conditions were established according to the instructions of Applied Biosystems (Rotkreuz, Switzerland). The respective cDNA was used in duplicate as a template for the real-time PCR analysis with the ABI PRISM 7000 Sequence Detection System (Applied Biosystems). The thermal cycle profile was 95°C for 15 s and 60°C for 1 min, repeated 45 times. To detect genomic DNA contaminations, all analyses included minus reverse transcriptase samples as negative controls.

GAPDH expression levels were analyzed in all samples as a housekeeping gene to normalize expression between different samples and to monitor assay reproducibility. Relative quantification of all targets was calculated by the comparative cycle threshold method outlined by the manufacturer (User Bulletin No. 2; Applied Biosystems).

MMP-2/-9/-14 and GAPDH. TaqMan PCR primers and probes were designed by using the Primer-Express software (Applied Biosystems).[56,46] One microliter cDNA solution containing 50 ng of reverse-transcribed total RNA was added to 24 μl of PCR reaction mixture. Reaction mixtures were composed as follows: TaqMan Universal PCR Master Mix (Applied Biosystems; containing AmpliTaq Gold DNA Polymerase) final concentration 1×, and 300 nM Probe, 300 nM forward primer and 900 nM reverse primer for GAPDH, MMP-2[56,46] and MMP-9 assays, respectively, or 150 nM Probe, 400 nM forward primer and 400 nM reverse primer for MMP-14 assay, or 100 nM Probe, 300 nM forward primer and 300 nM reverse primer for the second MMP-2 assay.[33] The primer concentrations for each assay were determined previously following the Applied Biosystems manual.[56,46]

MMP-7/-8/-11/-12, TIMP-1/-2/-3, ADAM-17, TGF-β1 and meprin α/β. Assays-on-Demand Gene Expression Products were used as described in the manufacturer's protocol (Applied Biosystems).

Protein extraction from kidney tissues

Frozen half-kidneys were minced on a cold Petri dish and transferred into separate tubes. Thereafter, 1 ml of lysis buffer (0.1 M Tris-HCl containing 0.1% Tween 80, pH 7.5 and 1 μg/ml Leupeptine) per 50 mg of wet tissue was added to perform enzyme activity analyses. For Western blot analyses, proteins were extracted in 25 mM Tris-HCl, 50 mM NaCl, pH 8.0, supplemented with 1% deoxycholic acid, 1% nonidet-P40, and one tablet per 10 ml extracting buffer of protease inhibitor cocktail (Complete Mini EDTA free; Roche Diagnostics, Rotkreuz, Switzerland). After homogenization, samples were centrifuged twice at 10 000 *g* for 10 and 5 min, respectively, to remove cell debris. Extracted supernatants were stored at −20°C. Protein concentrations were determined using the BCA protein assay reagent kit (Pierce, Lausanne, Switzerland).

MMP-2 and MMP-9 activity

Activities of these two gelatinases in frozen kidney samples were analyzed by gelatin substrate zymography (MMP-2/-9) and fluorometry (MMP-2), exactly as previously described by us.[46,52,35] Note, homogenized samples were used as is and were not further concentrated before their analyses.

Western blot analyses of MMP-9/-12/-14, TIMP-2 and meprin α/β

Western blot analyses were performed as described previously with some minor changes.[35] Following two washes in Tris buffered saline with 0.1% Tween, the blots were incubated overnight at room temperature by gently shaking in Tris buffered saline with 0.1% Tween/3.5% dry milk containing monoclonal mouse anti-MMP-9, anti-MMP-14 or anti-TIMP-2 (dilutions 1:50, 1:25 or 1:100, respectively; Oncogene, Lucerne, Switzerland), or polyclonal goat

anti-mouse MMP-12 (dilution 1:200; Santa Cruz Biotechnology, Inc.) or polyclonal rabbit anti-human meprin α or β antibodies (1:1000). Note, anti-human meprin antibodies were obtained from E Sterchi and co-workers[57] and were shown to crossreact with mouse and rat meprin (E Sterchi, personal communication).

Subsequently, the blots were washed extensively in Tris buffered saline with 0.1% Tween for 1 h (4×15 min) and incubated with goat anti-mouse or goat anti-rabbit (donkey anti-goat for MMP-12) HRP-conjugated secondary antibody. Finally, the membranes were incubated with enhanced chemiluminescent reagents for 5 min (Amersham Pharmacia Biotech, Dübendorf, Switzerland), followed by exposure to Hyperfilm enhanced chemiluminescent (Amersham Pharmacia Biotech). The molecular weight of the bands of interest was determined by a precision molecular weight marker from Biorad (Reinach, Switzerland).

Immunohistology of MMP-2 and MMP-9

Immunohistochemistry of MMP-2/-9 was performed using the rat renal cortex, as described previously.[35]

Immunohistology of meprin α and meprin β

The 2–3 μm paraffin-embedded kidney sections were dewaxed, rehydrated and pretreated by boiling in 10 mM citrate buffer, pH 5.65, in a microwave oven. Thereafter, and following all subsequent steps, sections were washed in Tris-buffered saline and blocked for 30 min with Tris-buffered saline containing 20% porcine serum. Samples were incubated for 35 min at room temperature with primary antibodies in Tris-buffered saline/5% porcine serum (rabbit anti-meprin α or anti-meprin β 1:2500). After washing 3 times for 10 min, sections were incubated for 35 min with biotinylated porcine-anti-rabbit immunoglobulin antiserum (dilution 1:300 from DakoCytomation, Glostrup, Denmark). Thereafter a streptavidin—biotin complex/alkaline phosphatase (1:50 in Tris-buffered saline) (DakoCytomation) was applied for 35 min. Sections were developed for 1 min in new fuchsin–levamisol (DakoCytomation), counterstained with hematoxylin (Merck, Dr Grogg Chemie, Stettlen-Deisswil, Bern, Switzerland) and finally mounted with Aquatex (Merck).

Meprin activity

Activity of meprin α and meprin β was assessed as outlined previously.[25] To measure total activity, a portion of the samples obtained from protein extraction described above was activated at 37°C for 2 h with 20 μg/ml trypsin. Before the meprin activity assay, trypsin was inhibited with 50 μg/ml of soybean trypsin inhibitor (Sigma, Dr Grogg Chemie, Stettlen-Deisswil, Bern, Switzerland). Meprin activity was measured using the *N*-benzoyl-L-tyrosyl-*p*-aminobenzoic acid[24] as substrate. After incubating samples at 37°C for 4 h with substrate (1:1, v/v), the reaction was stopped by the addition of 400 μl of 10% trichloroacetic acid. Precipitated proteins were removed by centrifugation. The *p*-amino-benzoic acid contained in 100 μl of cleared supernatant was subjected to a colorimetric reaction according to Bratton-Marshall by the addition of 200 μl of $NaNO_2$, 200 μl of ammonium sulfamate and 500 μl *N*-(naphtyl)-ethylene diamine. Photometric readings were taken at 546 nm including a standard solution of known benzoic acid concentration, and results were expressed as μmol/ml/h/mg of total protein.

Statistical analysis

The differences between mean values were analyzed by non-parametric Mann–Whitney test for variables that were not normally distributed. Results were confirmed by the one-way analysis of variance Kruskal–Wallis test. All statistical tests were two sided. Only the analyses of MMP-7 and MMP-8 were performed using the unpaired *t*-test.

Statistical analysis was performed with the GraphPad Prism Software version 3.02 for Windows (Graphpad Software, San Diego, CA, USA). Results are given as mean $\pm$ s.e.m. for continuous variables. Microarray and real-time PCR results were expressed as mean $\pm$ s.d., as described previously.[46] For all experiments, probability of error (*P*-values) was calculated. Values for $P < 0.05$ were regarded as significant.

Genechip MAS5 normalized expression values were subjected to analysis of variance and Kruskal–Wallis group statistical analyses. Further analyses were performed by GeneSpring 6.1.1 (Silicon Genetics).

ACKNOWLEDGMENTS

We are particularly thankful to Dr N Hartmann (Genomics Factory, Novartis Pharma AG, Basel, Switzerland), for having performed the Affymetrix microarray hybridizations. This work was supported by the Swiss National Foundation for Scientific Research by Grants NFP-46 (Hans-Peter Marti) and 3100A0-100772 (Erwin Sterchi). We also thank Dr P Wahl from our institution for correction of the manuscript.

Portions of this study were published as an abstract (*J Am Soc Nephrol* 2003; **14**: 423A) and were presented at the 36th Annual Meeting of the American Society of Nephrology, San Diego, CA, 2003.

REFERENCES

1. Cardarelli F, Saidman S, Theruvath T *et al.* The problem of late allograft loss in kidney transplantation. *Minerva Urol Nefrol* 2003; **55**: 1–11.
2. Racusen LC, Solez K, Colvin RB *et al.* The Banff 97 working classification of renal allograft pathology. *Kidney Int* 1999; **55**: 713–723.
3. Lovett DH, Johnson RJ, Marti HP *et al.* Structural characterization of the mesangial cell type IV collagenase and enhanced expression in a model of immune complex-mediated glomerulonephritis. *Am J Pathol* 1992; **141**: 85–98.
4. Turck J, Pollock AS, Lee LK *et al.* Matrix metalloproteinase 2 (gelatinase A) regulates glomerular mesangial cell proliferation and differentiation. *J Biol Chem* 1996; **271**: 15074–15083.
5. Carmago S, Shah SV, Walker PD. Meprin, a brush-border enzyme, plays an important role in hypoxic/ischemic acute renal tubular injury in rats. *Kidney Int* 2002; **61**: 959–966.
6. Norman LP, Jiang W, Han X *et al.* Targeted disruption of the meprin beta gene in mice leads to underrepresentation of knockout mice and changes in renal gene expression profiles. *Mol Cell Biol* 2003; **23**: 1221–1230.
7. Bertenshaw GP, Norcum MT, Bond JS. Structure of homo- and hetero-oligomeric meprin metalloproteinases. *J Biol Chem* 2003; **278**: 2522–2532.
8. Killar L, White J, Black R, Peschon J. Adamalysins. A family of metzincins including TNF-alpha converting enzyme (TACE). *Ann N Y Acad Sci* 1999; **878**: 442–452.
9. Duffy MJ, Lynn DJ, Lloyd AT, O'Shea CM. The ADAM family of proteins: from basic studies to potential clinical applications. *Thromb Haemost* 2003; **89**: 622–631.
10. Birkedal-Hansen H. Proteolytic remodeling of extracellular matrix. *Curr Opin Cell Biol* 1995; **7**: 728–735.
11. Cuvelier A, Kuntz C, Sesboue R *et al.* Les métalloprotéinases de la matrice extracellulaire (MMP): structure et activité. *Rev Mal Resp* 1997; **14**: 1–10.
12. Laplante A, Liu D, Demeule M *et al.* Modulation of matrix gelatinases and metalloproteinase-activating process in acute kidney rejection. *Transpl Int* 2003; **16**: 262–269.
13. Southgate KM, Davies M, Booth RFG, Newby AC. Involvement of extracellular-matrix-degrading metalloproteinases in rabbit aortic smooth-muscle cell proliferation. *Biochem J* 1992; **288**: 93–99.
14. Kitamura M, Shirasawa T, Maruyama N. Gene transfer of metalloproteinase transin induces aberrant behavior of cultured mesangial cells. *Kidney Int* 1994; **45**: 1580–1586.

15. Brew K, Dinakarpandian D, Nagase H. Tissue inhibitors of metalloproteinases: evolution, structure and function. *Biochim Biophys Acta* 2000; **1477**: 267–283.
16. Conway JG, Wakefield JA, Brown RH *et al.* Inhibition of cartilage and bone destruction in adjuvant arthritis in the rat by a matrix metalloproteinase inhibitor. *J Exp Med* 1995; **182**: 449–457.
17. Gijbels K, Galdary RE, Steinmann L. Reversal of experimental autoimmune encephalomyelitis with a hydroxamate inhibitor of matrix metalloproteinases. *J Clin Invest* 1994; **94**: 2177–2182.
18. Lelongt B, Trugnan G, Murphy G, Ronco PM. Matrix metalloproteinases MMP2 and MMP9 are produced in early stages of kidney morphogenesis but only MMP9 is required for renal organogenesis *in vitro*. *J Cell Biol* 1997; **136**: 1363–1373.
19. Hill PA, Docherty JP, Bottomley KM *et al.* Inhibition of bone resorption *in vitro* by selective inhibitors of gelatinase and collagenase. *Biochem J* 1995; **308**: 167–175.
20. Leppert D, Lindberg RL, Kappos L, Leib SL. Matrix metalloproteinases: multifunctional effectors of inflammation in multiple sclerosis and bacterial meningitis. *Brain Res Rev* 2001; **36**: 249–257.
21. Sanceau J, Truchet S, Bauvois B. Matrix metalloproteinase-9 silencing by RNA interference triggers the migratory-adhesive switch in Ewing's sarcoma cells. *J Biol Chem* 2003; **278**: 36537–36546.
22. Villa JP, Bertenshaw GP, Bond JS. Critical amino acids in the active site of meprin metalloproteinases for substrate and peptide bond specificity. *J Biol Chem* 2003; **278**: 42545–42550.
23. Kruse MN, Becker C, Lottaz D *et al.* Human meprin alpha and beta homo-oligomers: cleavage of basement membrane proteins and sensitivity to metalloprotease inhibitors. *Biochem J* 2004; **378**: 383–389.
24. Sterchi EE, Naim HY, Lentze MJ. Biosynthesis of *N*-benzoyl-L-tyrosyl-*p*-aminobenzoic acid hydrolase: disulfide-linked dimers are formed at the site of synthesis in the rough endoplasmic reticulum. *Arch Biochem Biophys* 1988; **265**: 119–127.
25. Kohler D, Kruse M, Stocker W, Sterchi EE. Heterologously overexpressed, affinity-purified human meprin α is functionally active and cleaves components of the basement membrane *in vitro*. *FEBS Lett* 2000; **465**: 2–7.
26. Kieran NE, Doran PP, Connolly SB *et al.* Modification of the transcriptomic response to renal ischemia/reperfusion injury by lipoxin analog. *Kidney Int* 2003; **64**: 480–492.
27. Trachtman H, Valderrama E, Dietrich JM, Bond JS. The role of meprin A in the pathogenesis of acute renal failure. *Biochem Biophys Res Commun* 1995; **208**: 498–505.
28. Doggrell SA. TACE inhibition: a new approach to treating inflammation. *Expert Opin Investig Drugs* 2002; **11**: 1003–1006.
29. Joosten SA, van Dixhoorn MGA, Borrias MC *et al.* Antibody response against perlecan and collagen types IV and VI in chronic renal allograft rejection in the rat. *Am J Pathol* 2002; **160**: 1301–1310.
30. Joosten SA, van Ham V, Nolan CE *et al.* Telomere shortening and cellular senescence in a model of chronic renal allograft rejection. *Am J Pathol* 2003; **162**: 1305–1312.
31. Racusen LC, Solez K, Colvin RB *et al.* The Banff 97 working classification of renal allograft pathology. *Kidney Int* 1999; **55**: 713–723.
32. Marti HP, McNeil L, Thomas G *et al.* Molecular characterization of a low-molecular-mass matrix metalloproteinase secreted by glomerular mesangial cells as PUMP-1. *Biochem J* 1992; **285**: 899–905.
33. Inaki N, Tsunezuka Y, Kawakami K *et al.* Increased matrix metalloproteinase-2 and membrane type 1 matrix metalloproteinase activity and expression in heterotopically transplanted murine tracheas. *J Heart Lung Transplant* 2004; **23**: 218–227.
34. Hernandez-Barrantes S, Toth M, Bernardo MM *et al.* Binding of active (57 kDa) membrane type-1 matrix metalloproteinase (MT1-MMP) to tissue inhibitor of metalloproteinase (TIMP)-2 regulates MT1-MMP processing and pro-MMP-2 activation. *J Biol Chem* 2000; **275**: 12080–12089.
35. Lods N, Ferrari P, Frey FJ *et al.* Angiotensin converting enzyme inhibition but not angiotensin II receptor blockade reduces matrix metalloproteinase activity in glomerulonephritis. *J Am Soc Nephrol* 2003; **14**: 2861–2872.
36. Lorenzl S, Albers DS, Relkin N *et al.* Increased plasma levels of matrix metalloproteinase-9 in patients with Alzheimer's disease. *Neurochem Int* 2003; **43**: 191–196.
37. Kjeldsen L, Johnsen AH, Sengelov H, Borregaard N. Isolation and primary structure of NGAL, a novel protein associated with human neutrophil gelatinase. *J Biol Chem* 1993; **268**: 10425–10432.
38. Eberhardt W, Beeg T, Beck KF *et al.* Nitric oxide modulates expression of matrix metalloproteinase-9 in rat mesangial cells. *Kidney Int* 2000; **57**: 59–69.
39. Takei I, Takagi M, Santavirta S *et al.* Matrix metalloproteinases and tissue inhibitors of metalloproteinases in joint fluid of the patients with loose artificial hip joints. *J Biomed Mater Res* 1999; **45**: 175–183.
40. Yang YN, Bauer D, Wasmuth S *et al.* Matrix metalloproteinases (MMP-2 and 9) and tissue inhibitors of matrix metalloproteinases (TIMP-1 and 2) during the course of experimental necrotizing herpetic keratitis. *Exp Eye Res* 2003; **77**: 227–237.
41. Lu KV, Jong KA, Rajasekaran AK *et al.* Upregulation of tissue inhibitor of metalloproteinases (TIMP)-2 promotes matrix metalloproteinase (MMP)-2 activation and cell invasion in a human glioblastoma cell line. *Lab Invest* 2004; **84**: 8–20.
42. Kaushal GP, Walker PD, Shah SV. An old enzyme with a new function: purification and characterization of a distinct matrix-degrading metalloproteinase in rat kidney cortex and its identification as meprin. *J Cell Biol* 1994; **126**: 1319–1327.
43. Johnson GD, Hersh LB. Expression of meprin subunit precursors. Membrane anchoring through the beta subunit and mechanism of zymogen activation. *J Biol Chem* 1994; **269**: 7682–7688.
44. Rodrigo E, López Hoyos M, Escallada R *et al.* Changes in serum concentrations of matrix metalloproteinases in kidney transplantation. *Transplant Proc* 2000; **32**: 517–518.
45. Rodrigo E, López-Hoyos M, Escallada R *et al.* Circulating levels of matrix metalloproteinases MMP-3 and MMP-2 in renal transplant patients with chronic transplant nephropathy. *Nephrol Dial Transplant* 2000; **15**: 2041–2045.
46. Ermolli M, Schumacher M, Lods N *et al.* Differential expression of MMP-2/MMP-9 and potential benefit of MMP inhibitor in experimental acute kidney allograft rejection. *Transplant Immunol* 2003; **11**: 137–145.
47. Saunders RN, Bicknell GR, Nicholson ML. The impact of cyclosporine dose reduction with or without the addition of rapamycin on functional, molecular, and histological markers of chronic allograft nephropathy. *Transplantation* 2003; **75**: 772–780.
48. Warner RL, Lewis CS, Beltran L *et al.* The role of metalloelastase in immune complex-induced acute lung injury. *Am J Pathol* 2001; **158**: 2139–2144.
49. Bax DV, Messent AJ, Tart J *et al.* Integrin alpha 5beta 1 and TNF-α converting enzyme (TACE/ADAM-17) interact *in vitro* and colocalise in migrating HeLa cells. *J Biol Chem* 2004 [E-pub ahead of print].
50. Rosmann S, Hahn D, Lottaz D *et al.* Activation of human meprin-alpha in a cell culture model of colorectal cancer is triggered by the plasminogen-activating system. *J Biol Chem* 2002; **277**: 40650–40658.
51. Ramont L, Pasco S, Hornebeck W *et al.* Transforming growth factor-beta1 inhibits tumor growth in a mouse melanoma model by down-regulating the plasminogen activation system. *Exp Cell Res* 2003; **291**: 1–10.
52. Steinmann-Niggli K, Küng M, Ziswiler R, Marti HP. Inhibition of matrix metalloproteinases attenuates anti-Thy1.1 nephritis. *J Am Soc Nephrol* 1998; **9**: 397–407.
53. Steinmann-Niggli K, Lukes M, Marti HP. Rat mesangial cells and matrix metalloproteinase inhibitor: Inhibition of 72-kDa type IV collagenase (MMP-2) and of cell proliferation. *J Am Soc Nephrol* 1997; **8**: 395–405.
54. Daniel C, Duffield J, Brunner T *et al.* Matrix metalloproteinase inhibitors cause cell cycle arrest and apoptosis in glomerular mesangial cells. *J Pharmacol Exp Ther* 2001; **297**: 57–68.
55. Szabo A, Lutz J, Schleimer K *et al.* Effect of angiotensin-converting enzyme inhibition on growth factor mRNA in chronic renal allograft rejection in the rat. *Kidney Int* 2000; **57**: 982–991.
56. Leib SL, Clements JM, Lindberg RL *et al.* Inhibition of matrix metalloproteinases and tumour necrosis factor α converting enzyme as adjuvant therapy in pneumococcal meningitis. *Brain* 2001; **124**: 1734–1742.
57. Lottaz D, Hahn D, Müller S *et al.* Secretion of human meprin from intestinal epithelial cells depends on differential expression of the α and β subunits. *Eur J Biochem* 1999; **259**: 496–504.